Turkish J. Eng. Env. Sci.
28 (2004) , 25 – 40.

Investigation of Hydrodynamic Effects on Linear and Nonlinear Earthquake Responses of Arch Dams by the Lagrangian Approach

Mehmet AKKÖSE
Karadeniz Technical University, Faculty of Engineering and Architecture, Department of Civil Engineering, Trabzon-TURKEY
akkose@ktu.edu.tr
A. Aydın DUMANOĞLU
Karadeniz Technical University, Faculty of Engineering and Architecture, Department of Civil Engineering, Trabzon-URKEY
aduman@ktu.edu.tr
M. Emin TUNA
Gazi University, Faculty of Engineering and Architecture, Department of Architecture, Ankara-TURKEY
mtuna@gazi.edu.tr

Received 07.01.2003

Abstract

The linear and nonlinear responses of a selected arch dam subjected to earthquake ground motion are presented in this study. The hydrodynamic effects on the dynamic response of arch dams are investigated using step-by-step integration by the Lagrangian approach. The foundation flexibility effects on dam response are also examined. Water in the reservoir was represented by 8-noded Lagrangian fluid finite elements. The element including compressible behavior and surface sloshing motion of the fluid has been coded and incorporated into a general-purpose computer program, NONSAP. In this study, the curve description method describes the nonlinear behavior of the dam concrete. The El-Centro N-S component of the Imperial Valley earthquake, on May 18, 1940, has been used as the ground motion. The response of the dam was characterized by crest displacements and envelopes of maximum tensile stresses.

Key words: Hydrodynamic effect, Dam-water-foundation interaction, Linear and nonlinear analysis, Curve description method, Earthquake responses.

Introduction

Dams are monolithic structures. The collapse of a dam due to an earthquake may cause extensive damage to property and loss of life on its downstream due to the sudden release of a large quantity of water.

When a dam-water system is subjected to an earthquake, hydrodynamic pressures that are in excess of the hydrostatic pressures occur on the upstream face of the dam due to the vibration of the dam and impounded water. Arch dams resist the major part of the hydrodynamic pressures and other loads by transmitting them through arch action to the canyon walls. Consequently, interaction between the dam and impounded water and interaction between the dam and foundation rock are two important factors affecting the dynamic response of arch dams during earthquake ground motion. The prediction of the actual dynamic response of an arch dam to earthquake loadings is a very complicated problem and depends on several factors, such as interaction of the dam with its foundation rock and reservoir water, and the computer modeling and material properties used in the analysis. Therefore, an

efficient method is required to properly assess the safety of an arch dam located in regions with significant seismicity. From this point of view, linear and nonlinear dynamic analyses of arch dams for earthquake ground motions should be based on a detailed analytical model. Furthermore, this model should be capable of correctly representing both the materially linear and nonlinear behavior and the 3-dimensional nature of the dam-water-foundation system, which account for the interaction effects of the foundation rock and the impounded water. To compute the linear and nonlinear response, the concrete arch and the foundation rock are modeled by standard finite elements, whereas the interaction effects of the impounded water can be represented by any of three basic approaches. The simplest is the added mass attached to the dam (Westergaard, 1933). Another approach describing the dam-water interaction is the Eulerian. In this approach, displacements are the variable in the structures; whereas pressures are that of the fluid. Since the variables in the fluid and structure are different in the approach, a special-purpose computer program for the solution of coupled systems is required. The Lagrangian approach is a third way to the fluid-structure interaction solution. In this approach, the behavior of fluid and structure are expressed in terms of displacements. Since available general-purpose structural analysis programs use the displacements to obtain the response of the structures, Lagrangian displacement-based fluid elements can easily be incorporated into the programs. This is the most important advantage of the approach. However, this causes some numerical problems. The disadvantage of the displacement-based fluid element is related to the mode superposition method. The modal analysis of fluid or fluid-structure systems yields some spurious zero energy modes. Many researchers have focused on improving various fluid elements that may eliminate the numerical problem (Chopra *et al.*, 1969; Shugar and Katona, 1975; Hamdi *et al.*, 1978; Zienkiewicz and Bettess, 1978; Akkaş *et al.*, 1979; Wilson and Khalvati, 1983;).

Chopra *et al.* (1969), Shugar and Katona (1975) and Akkaş *et al.* (1979) idealized the fluid as a structural finite element with zero shear modulus. Akkaş *et al.* (1979) showed that the direct integration method gave reliable results in their study. Zienkiewicz and Bettess (1978) gave a general description of the approaches used in the solution of coupled fluid-solid systems. They suggested the addition of a small but finite shear modulus to eliminate the spurious zero energy modes. Hamdi *et al.* (1978) introduced global rotational constraints in order to correct these spurious modes. Wilson and Khalvati (1983) proposed the reduced integration technique together with rotational constraints to produce a single element stiffness matrix and to optimize the behavior of the fluid mesh. Thus, all spurious zero energy modes were eliminated. Many researchers used the Lagrangian fluid elements that were improved by Wilson and Khalvati (1983) in 2-dimensional fluid, fluid-structure and dam-water interaction problems (Greeves, 1991; Calayır and Dumanoğlu, 1993; Calayır, 1994; Calayir *et al.*, 1996). In these studies, it is generally reported that the Lagrangian fluid elements give satisfactory results using a step-by-step integration method.

In previous investigations on the earthquake response of arch dams, the complex frequency functions have generally been used to define dam-water and dam-foundation rock interactions (Perumalswami and Kar, 1973; Fok and Chopra, 1986; Tan and Chopra, 1995, 1996). They have shown that the dynamic response of arch dams to earthquake ground motions is affected by these interactions. The purpose of this study is the investigation of hydrodynamic effects on linear and nonlinear earthquake responses of a selected arch dam using a step-by-step integration technique with a Lagrangian approach. To that end, an 8-noded 3-dimensional Lagrangian fluid finite element put forward by Wilson and Khalvati (1983) was coded by the authors in the language FORTRAN 77 and incorporated into the general linear and nonlinear finite element computer program, NONSAP (Bathe *et al.*, 1974). In this study, the stress-strain curve of the dam concrete was idealized as being elasto-plastic. For this reason, the nonlinear material model referred to as the curve description available in NONSAP (Bathe *et al.*, 1974) was used.

Equations of Motion Based on the Lagrangian Approach

The equations of motion are first given for the fluid systems. Then the equations of motion of the fluid-structure system will be provided.

Only fluid system: In the Lagrangian approach, fluid is assumed to be linear-elastic, inviscid and irrotational. For this fluid, the relationship between pressures and volumetric strain is given by

$$P = C_{11}\,\varepsilon_v \tag{1}$$

where P, C_{11} and ε_v are the pressures that are equal to mean stresses, the bulk modulus and the volumetric strains of the fluid, respectively. The volumetric strain, ε_v, can be expressed in terms of the Cartesian displacement components as follows

$$\varepsilon_v = \frac{\partial U_{fx}}{\partial x} + \frac{\partial U_{fy}}{\partial y} + \frac{\partial U_{fz}}{\partial z} \tag{2}$$

where U_{fx},U_{fy} and U_{fz} are the displacement components in the Cartesian axes x, y and z, respectively.

The irrotationality of the fluid is considered like penalty methods (Zienkiewicz and Taylor, 1989; Bathe, 1996). Therefore, rotations and constraint parameters are included in the stress-strain equations of the fluid. These rotations are defined by

$$\begin{aligned} w_x &= \frac{1}{2}\left(\frac{\partial U_{fy}}{\partial z} - \frac{\partial U_{fz}}{\partial y}\right) \\ w_y &= \frac{1}{2}\left(\frac{\partial U_{fz}}{\partial x} - \frac{\partial U_{fx}}{\partial z}\right) \\ w_z &= \frac{1}{2}\left(\frac{\partial U_{fx}}{\partial y} - \frac{\partial U_{fy}}{\partial x}\right) \end{aligned} \tag{3}$$

where w_x, w_y and w_z are the rotations about the Cartesian axes x, y and z, respectively. The relationship between stress and stiffness (constraint parameters) associated with these rotations may be expressed as

$$\begin{aligned} P_x &= C_{22} w_x \\ P_y &= C_{33} w_y \\ P_z &= C_{44} w_z \end{aligned} \tag{4}$$

where P_x, P_y, P_z are the rotational stresses and C_{22}, C_{33}, C_{44} are the constraint parameters.

For a general 3-dimensional fluid element, stress-strain relationships can be written by using Eqs. (1) and (4) in matrix form as follows

$$\begin{Bmatrix} P \\ P_x \\ P_y \\ P_z \end{Bmatrix} = \begin{bmatrix} C_{11} & 0 & 0 & 0 \\ 0 & C_{22} & 0 & 0 \\ 0 & 0 & C_{33} & 0 \\ 0 & 0 & 0 & C_{44} \end{bmatrix} \begin{Bmatrix} \varepsilon_v \\ w_x \\ w_y \\ w_z \end{Bmatrix} \tag{5}$$

or

$$\sigma_f = \mathbf{C}_f \mathbf{e}_f \tag{6}$$

where σ_f and $\mathbf{e}_f$ are the stress and strain vectors of the fluid, respectively. $\mathbf{C}_f$ is the elasticity matrix of the fluid.

In the study, the equations of motion of the fluid system are obtained using energy principles. Using the finite element approximation, the total strain energy of the fluid system may be written as

$$\pi_e = \frac{1}{2}\mathbf{U}_f^T \mathbf{K}_f \mathbf{U}_f \tag{7}$$

where $\mathbf{U}_f$ and $\mathbf{K}_f$ are the nodal displacement vector and the stiffness matrix of the fluid system, respectively. Similarly, the free surface potential energy is expressed as

$$\pi_s = \frac{1}{2}\mathbf{U}_{sf}^T \mathbf{S}_f \mathbf{U}_{sf} \tag{8}$$

where $\mathbf{U}_{sf}$ and $\mathbf{S}_f$ are the vertical nodal displacement vector and stiffness matrix of the free surface of the fluid system, respectively. In addition, the kinetic energy of the system can be written as

$$T = \frac{1}{2}\dot{\mathbf{U}}_f^T \mathbf{M}_f \dot{\mathbf{U}}_f \tag{9}$$

where $\dot{\mathbf{U}}_f$ and $\mathbf{M}_f$ are the nodal velocity vector and the mass matrix of the fluid system, respectively. If Eqs. (7), (8) and (9) are combined using the Lagrange equation, the following set of equations is obtained:

$$\mathbf{M}_f \ddot{\mathbf{U}}_f + \mathbf{K}_f \mathbf{U}_f + \mathbf{S}_f \mathbf{U}_{sf} = \mathbf{R}_f \tag{10}$$

or

$$\mathbf{M}_f \ddot{\mathbf{U}}_f + \mathbf{K}_f^* \mathbf{U}_f = \mathbf{R}_f \tag{11}$$

where $\mathbf{K}_f^*$, $\ddot{\mathbf{U}}_f$ and $\mathbf{R}_f$ are the system stiffness matrix including the free surface stiffness, the nodal acceleration vector and the time-varying nodal force vector for the fluid system, respectively. In the formation of the fluid element matrices, reduced integration orders were utilized. The 8-noded 3-dimensional fluid element was used in the finite element model of the fluid system. For this element, the reduced integration order is (1x1x1).

Coupled fluid-structure system: The equations of motion of the fluid system, Eq. (11), have a similar form to those of the structure system. To obtain the coupled equations of the fluid-structure system, a determination of the interface condition is required. Since the fluid is assumed to be inviscid, only the displacement in the normal direction to the interface is continuous at the interface of the system. Assuming that the positive face is the structure and the negative face is the fluid, the boundary condition at the fluid-structure interface is

$$U_n^- = U_n^+ \tag{12}$$

where U_n is the normal component of the interface displacement (Akkaş *et al.*, 1979). Using the interface condition, the equations of motion of the coupled system to ground motion including damping effects are given by

$$\mathbf{M}_c\ddot{\mathbf{U}}_c + \mathbf{C}_c\dot{\mathbf{U}}_c + \mathbf{K}_c\mathbf{U}_c = -\mathbf{M}_c\mathbf{a}_g \tag{13}$$

in which $\mathbf{M}_c$, $\mathbf{C}_c$ and $\mathbf{K}_c$ are the mass, damping and stiffness matrices for the coupled system. $\mathbf{U}_c$, $\dot{\mathbf{U}}_c$ and $\ddot{\mathbf{U}}_c$ are the vectors of the displacement, velocity and acceleration of the coupled system. $\mathbf{a}_g$ is the vector of ground acceleration.

Step-by-Step Solution of Equations of Motion

The incremental equation of motion of Eq. (13) given for general dynamic fluid-structure systems can be written as

$$\mathbf{M}\Delta\ddot{\mathbf{U}}_i + \mathbf{C}\Delta\dot{\mathbf{U}}_i + \mathbf{K}_i\Delta\mathbf{U}_i = \Delta\mathbf{P}_i \tag{14}$$

where $\mathbf{M}$ and $\mathbf{C}$ are the constant mass and damping matrix, respectively. The constant damping matrix, $\mathbf{C}$, is calculated by applying Rayleigh damping coefficients to the constant mass matrix, $\mathbf{M}$, and the linear stiffness matrix, $\mathbf{K}$, of the system (Bathe *et al.*, 1974). $\mathbf{K}_i$ is the stiffness matrix in the ith time step. $\Delta\ddot{\mathbf{U}}_i$, $\Delta\dot{\mathbf{U}}_i$, $\Delta\mathbf{U}_i$ and $\Delta\mathbf{P}_i$ are the incremental acceleration, velocity, displacement and external load vectors in the ith time step, respectively. Using the linear acceleration method, the incremental velocity and displacement can be written as follows:

$$\Delta\dot{\mathbf{U}}_i = (\Delta t)\ddot{\mathbf{U}}_i + \frac{\Delta t}{2}\Delta\ddot{\mathbf{U}}_i \tag{15}$$

$$\Delta\mathbf{U}_i = (\Delta t)\dot{\mathbf{U}}_i + \frac{(\Delta t)^2}{2}\ddot{\mathbf{U}}_i + \frac{(\Delta t)^2}{6}\Delta\ddot{\mathbf{U}}_i \tag{16}$$

The linear acceleration method is conditionally stable. The Wilson-θ method developed by E.L. Wilson makes it unconditionally stable (Chopra, 1995). In this method, the time increment, Δt, is extended as follows

$$\delta t = \theta\Delta t \tag{17}$$

If Δt is replaced by δt and the incremental responses in Eqs. (15) and (16) are replaced by $\delta\mathbf{U}_i$, $\delta\dot{\mathbf{U}}_i$ and $\delta\ddot{\mathbf{U}}_i$, these equations can be rewritten as

$$\delta\dot{\mathbf{U}}_i = (\delta t)\ddot{\mathbf{U}}_i + \frac{\delta t}{2}\delta\ddot{\mathbf{U}}_i \tag{18}$$

$$\delta\mathbf{U}_i = (\delta t)\dot{\mathbf{U}}_i + \frac{(\delta t)^2}{2}\ddot{\mathbf{U}}_i + \frac{(\delta t)^2}{6}\delta\ddot{\mathbf{U}}_i \tag{19}$$

From Eq. (19)

$$\delta\ddot{\mathbf{U}}_i = \frac{6}{(\delta t)^2}\delta\mathbf{U}_i - \frac{6}{\delta t}\dot{\mathbf{U}}_i - 3\ddot{\mathbf{U}}_i \tag{20}$$

If Eq. (20) is substituted into Eq. (18), then

$$\delta\dot{\mathbf{U}}_i = \frac{3}{\delta t}\delta\mathbf{U}_i - 3\dot{\mathbf{U}}_i - \frac{\delta t}{2}\ddot{\mathbf{U}}_i \tag{21}$$

Next, Eqs. (20) and (21) are substituted into the incremental equation of motion over the extended time increment:

$$\mathbf{M}\delta\ddot{\mathbf{U}}_i + \mathbf{C}\delta\dot{\mathbf{U}}_i + \mathbf{K}_i\delta\mathbf{U}_i = \delta\mathbf{P}_i \tag{22}$$

where the external load vector also varies linearly over the extended time increment as follows (Chopra, 1995):

$$\delta\mathbf{P}_i = \theta(\Delta\mathbf{P}_i) \tag{23}$$

The accuracy and stability properties of the method depend on the value of the parameter θ, which is always greater than 1. The equation solved in each time increment can be written as follows

$$\hat{\mathbf{K}}_i \delta \mathbf{U}_i = \delta \hat{\mathbf{P}}_i \tag{24}$$

where

$$\hat{\mathbf{K}}_i = \mathbf{K}_i + \frac{3}{\theta\,\Delta t}\mathbf{C} + \frac{6}{(\theta \Delta t)^2}\mathbf{M} \tag{25}$$

$$\begin{aligned} \delta \hat{\mathbf{P}}_i = \theta\,(\Delta \mathbf{P}_i) \quad & +(\tfrac{6}{\theta \Delta t}\mathbf{M} + 3\mathbf{C})\,\dot{\mathbf{U}}_i \\ & +(3\mathbf{M} + \tfrac{\theta \Delta t}{2}\mathbf{C})\,\ddot{\mathbf{U}}_i \end{aligned} \tag{26}$$

Eq. (24) is solved for $\delta \mathbf{U}_i$, and $\delta \ddot{\mathbf{U}}_i$ is computed from Eq. (20). The incremental acceleration over the normal time increment is given by

$$\Delta \ddot{\mathbf{U}}_i = \frac{1}{\theta}\delta \ddot{\mathbf{U}}_i \tag{27}$$

and incremental velocity and displacement are determined from Eqs. (15) and (16), respectively. For the next time step displacement, velocity, and acceleration are calculated by

$$\left.\begin{aligned} \mathbf{U}_{i+1} &= \mathbf{U}_i + \Delta \mathbf{U}_i \\ \dot{\mathbf{U}}_{i+1} &= \dot{\mathbf{U}}_i + \Delta \dot{\mathbf{U}}_i \\ \ddot{\mathbf{U}}_{i+1} &= \ddot{\mathbf{U}}_i + \Delta \ddot{\mathbf{U}}_i \end{aligned}\right\} \tag{28}$$

and other procedures are continuous during the total solution time.

Nonlinear Material Model

Concrete capable of displaying nonlinear characteristics is an essential material in many structures, such as arch dams. The stress-strain curve of concrete depends on many factors. Consequently, defining material behavior correctly is very difficult. For efficient solutions, models representing the behavior of concrete in the best possible manner are required. The stress-strain relationship of concrete can be idealized by various simplifications and assumptions. The nonlinear material model used to represent concrete behavior in this study is the curve description model, which describes an isotropic hypoelastic material law, in which the bulk and shear moduli are functions of the stress and strain invariants. An explicit yield condition is not used, and whether the material is under loading and unloading is determined by the history of the volume strain only. That is, the functional relationships are used to replace an explicit yield condition (Bathe *et al.*, 1974).

The curve description model describing the instantaneous bulk and shear moduli as a piecewise linear function of the current volume strain is a simple incremental stress-strain law (Figure 1). The incremental stress-strain relations considered in the solution are assumed to be

$$s_{ij} = 2G g_{ij} \tag{29}$$

and

$$\sigma_m = 3K e_m \tag{30}$$

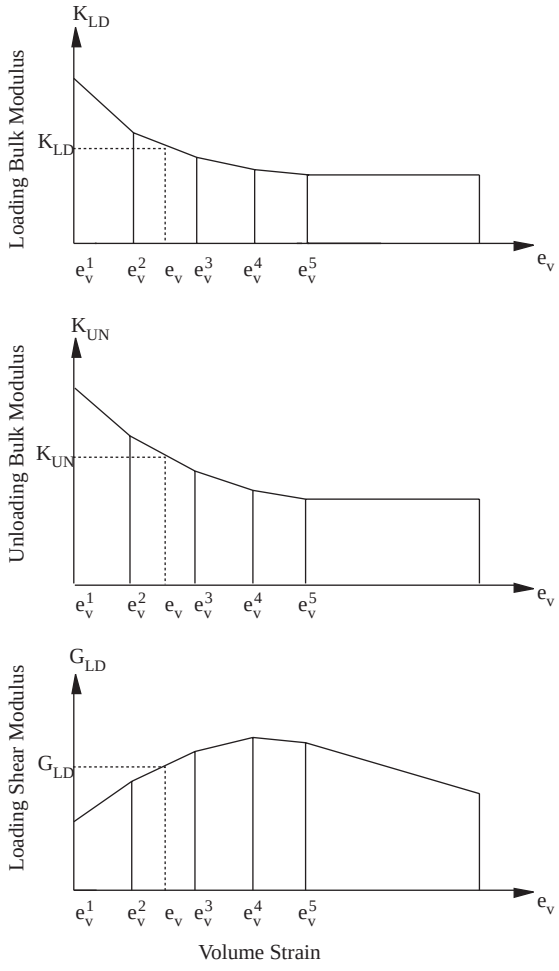

Figure 1. Moduli versus volume strain for the curve description model (Bathe *et al.*, 1974).

where s_{ij} and g_{ij} are the incremental deviatoric stresses and strains, and σ_m and e_m are the incremental mean stress and strain. The bulk (K) and shear (G) moduli can be expressed in terms of the elastic constants E and ν as follows

$$K = \frac{E}{3(1-2\nu)} \text{ and } G = \frac{E}{2(1+\nu)} \tag{31}$$

Defining $e_{\min}$ as the minimum mean strain reached during the solution, the material is loading if $e_m \leq e_{\min}$ and the material is unloading if $e_m > e_{\min}$, i.e.

$$K = \begin{cases} e_m \leq e_{\min} & ise \quad K_{LD} \\ e_m > e_{\min} & ise \quad K_{UN} \end{cases} \tag{32}$$

and

$$G = \begin{cases} e_m \leq e_{\min} & ise \quad G_{LD} \\ e_m > e_{\min} & ise \quad G_{UN} \end{cases} \tag{33}$$

The loading conditions for both the bulk and the shear moduli are determined by the history of e_m only. Six volumetric strain values are used to characterize the history of the material as shown in Figure 1. The bulk and shear moduli corresponding to the six volume strains are determined using the stress-strain relation assumed. Linear interpolation is used to obtain the loading (K_{LD}) and unloading (K_{UN}) bulk moduli and the loading shear modulus (G_{LD}) at any time. The unloading shear modulus (G_{UN}) is obtained as follows

$$G_{UN} = G_{LD}\frac{K_{UN}}{K_{LD}} \tag{34}$$

Although it is used to represent the response of geological materials, in this study the curve description model represents the behavior of dam concrete. The loading and unloading bulk moduli and the loading shear modulus for concrete material are determined using the elasto-plastic stress-strain relationship given in Figure 2.

Numerical Applications and Discussion

Dam-water-foundation rock system and ground motion

The arch dam selected for this study is Type-5 as suggested in the symposium on arch dams (ICE, 1968), in London. The view in plan and the vertical crown cross section of the arch dam is shown in Figure 3. The dimensions of the arch dam are in units. The height was chosen as 120 m to obtain realistic results. The other dimensions of the dam were determined according to this size. The finite element idealizations prepared for the dam, dam-water and dam-water-foundation rock systems are presented in Figures 4 and 5, respectively. The depth of the reservoir is 120 m and its length was taken as 3 times its depth. Eight-noded 3-dimensional solid elements were used to represent the dam and foundation rock. The number of elements in the dam is 128, and that in the foundation rock is 164. To represent the water in the reservoir, 512 8-noded 3-dimensional fluid elements were used. Fluid is assumed to transmit normal forces to its boundary because of its inviscid nature. The boundary condition on many fluid-structure systems was achieved by the use of con-

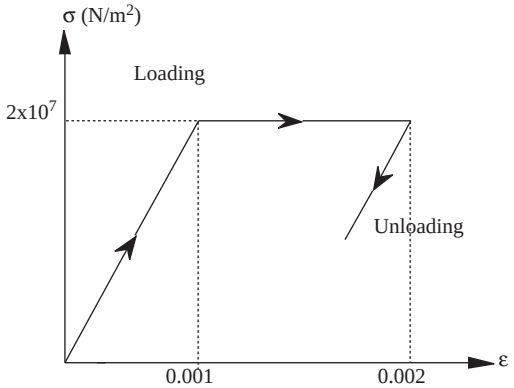

Figure 2. The stress-strain relationship assumed for dam concrete.

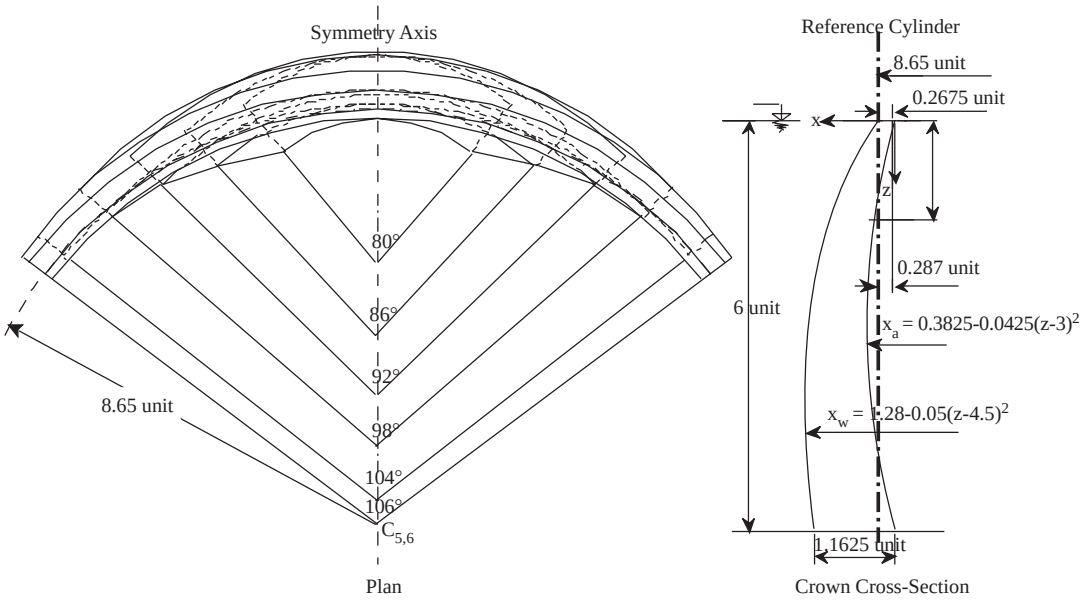

Level	C_0	C_1	C_2	C_3	C_4	C_5	C_6
Radius (unit)	3.67	5.29	6.64	7.72	8.54	8.80	8.50
Central Angle	80 °	86 °	92 °	98 °	104 °	106 °	106 °

Figure 3. The view in plan and the vertical crown cross section of Type-5 arch dam (ICE, 1968).

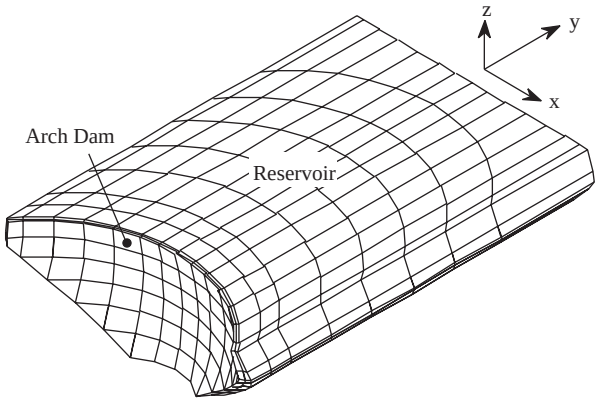

Figure 4. The finite element model of dam-water interaction system of Type-5 arch dam.

straint relations (Calayir *et al.*, 1996; Greeves, 1991; Olson and Bathe, 1983; Zienkiewicz and Bettess, 1978). Due to the complex geometry of the arch dam and its reservoir, short and axially almost rigid truss elements in the direction of the interface used by Akkaş *et al.* (1979) were used instead of constraints relations. The rigid truss elements were introduced between the grounded nodes and their corresponding fluid nodes. The grounded nodes were completely restrained. In this way complete tangential motion of the fluid to the dam and canyon was still possible. For this reason, a total of 122 truss elements were utilized at the interfaces of the dam and the water, and of the water and canyon. The length and the elasticity modulus of the truss elements were taken as 0.001 m and 2×10^{16} N/m^2, respectively. There are a total of 969 nodal points in the dam-water system (Figure 4), and 1374 nodal points in the dam-water-foundation rock system (Figure 5). A 2-dimensional view of the finite element mesh of the dam-water-foundation rock system at the vertical crown section is shown in Figure 6. At the boundaries of the dam-water and the dam-water-foundation rock systems there are 560 and 518 restrained degrees of freedom,

respectively. Hence, these representations lead to 2347 and 3604 active degrees of freedom (or equations) in total, respectively.

The material properties of the dam-water-foundation rock system for this study are as follows; for the linear behavior of the dam concrete, elasticity modulus, mass density and Poisson's ratio were taken as 2×10^{10} N/m^2, 2446.48 kg/m^3 and 0.15, respectively. For the elasto-plastic behavior of the dam concrete, the stress-strain relationship is given in Figure 2. The foundation rock was assumed to be linearly elastic. Its elasticity modulus, mass density and Poisson's ratio were taken as 1.379×10^{10} N/m^2, 2689.09 kg/m^3 and 0.24, respectively. The fluid was assumed to be linearly elastic, inviscid and irrotational. The bulk modulus and mass density of the fluid were taken as 0.207×10^{10} N/m^2 and 1000 kg/m^3, respectively. The rotation constraint parameters of the fluid about each Cartesian axis were taken as 1000 times those of the bulk modulus.

Two methods for the solution of the equations of motion are available: direct integration and mode superposition. In the direct integration method, step-by-step integration is applied to the original equations of motion with no transformation being carried out to uncouple them. The direct integration method is most effective when the response is required for a relatively short duration, as in this study. The step-by-step integration technique, the Wilson-θ method, was used for the solution in this study. The solution time step chosen was 0.0025 s for the integration. This method requires that the damping matrix to be represented be in explicit form. This is accomplished by using Rayleigh damping (Bathe, 1996; Chopra, 1995; Clough and Penzien, 1993). If there are two different domains in the system, such as fluid and structure, the damping matrix for the complete system is constructed by directly assembling the damping matrices for the two subsystems (Bathe, 1996; Chopra, 1995; Clough and Penzien, 1993). The damping matrices for the structure and the fluid are

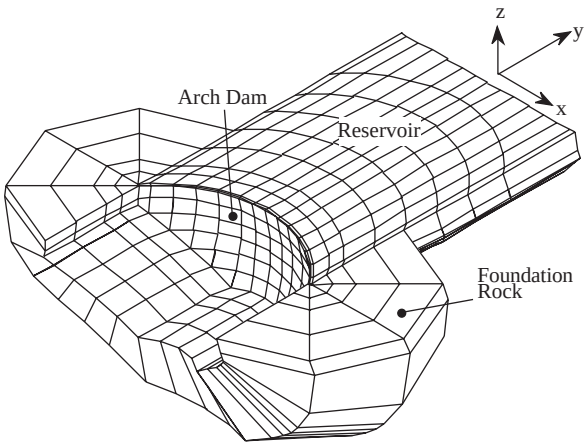

Figure 5. The finite element model of dam-water-foundation interaction system of Type-5 arch dam.

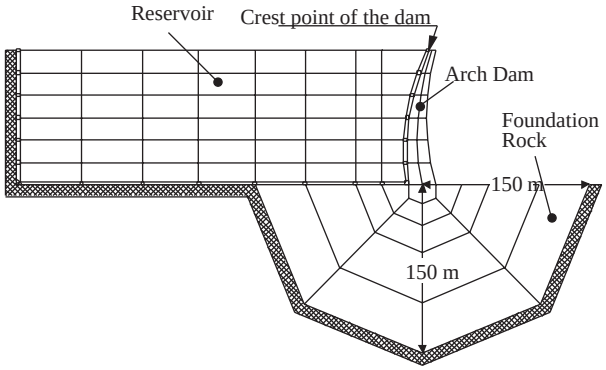

Figure 6. 2-dimensional view of finite element mesh of dam-water-foundation interaction system at the vertical crown section.

$$\mathbf{C}_s = a_0\mathbf{M}_s + a_1\mathbf{K}_s \text{ (for structure)} \qquad (35)$$

$$\mathbf{C}' = a_0'\mathbf{M}_f + a_1'\mathbf{K}_f \text{ (for fluid)} \qquad (36)$$

where coefficients a_0 and a_1 obtained from two given damping ratios associated with two frequencies of vibration. If both frequencies are assumed to have the same damping ratio (ξ), then a_0 and a_1 constants can be obtained by (Bathe, 1996; Chopra, 1995; Clough and Penzien, 1993)

$$a_0 = \xi\frac{2\omega_i\omega_j}{\omega_i+\omega_j} \text{ and } a_1 = \xi\frac{2}{\omega_i+\omega_j} \qquad (37)$$

where ω_i and ω_j are the i^{th} and j^{th} mode frequencies of the system, respectively. The coefficients a_0' and a_1' are determined similarly, using an appropriate damping ratio for the fluid domain. In this study, Rayleigh damping constants were taken to be the same values for both fluid and structure. The damping constants were calculated within a frequency range of the natural frequency of the first bending mode of the dam-water and the dam-water-foundation rock systems to 10 Hz, assuming a 5% damping ratio.

The El-Centro N-S component of the Imperial Valley earthquake on May 18, 1940, measured on a rock-like surface was chosen for the ground motion. The component considered was applied in the upstream-downstream direction. In the analysis only the first 6.5 s of the earthquake were used.

Response results

A Type-5 arch dam was analyzed to identify the effects of impounded water on the linear and nonlinear response using the curve description method of the dam subjected to El-Centro earthquake ground motion for the dam on both rigid and flexible foundation rock with both an empty and a full reservoir. The response results presented to illustrate the hydrodynamic effects in this study consist of displacement time-history and contours of maximum tensile stresses in each Cartesian axis for the upstream dam faces. It is useful to display the maximum tensile stresses in the form of contour plots for dam faces. That is, because the maximum tensile stresses represent the largest computed tensile stresses at all locations in the dam during earthquake ground motion. The maximum tensile stresses at different points are generally reached at different times. Contour plots of the maximum tensile stresses provide a convenient means for identifying the overstressed areas.

Response of the Type-5 arch dam on rigid foundation rock

The time-history of displacements obtained from the linear analysis of the dam at the crest of the Type-5 arch dam on rigid foundation rock with both an empty and a full reservoir is shown in Figure 7(a),

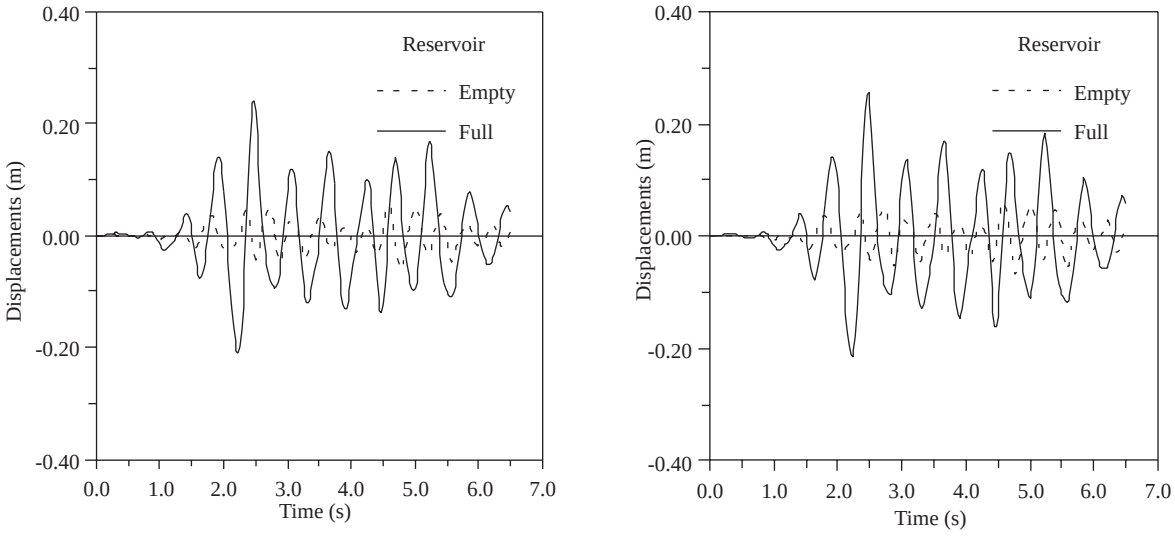

(a) Linear Analysis (b) Nonlinear Analysis

Figure 7. The time history of displacements at the crest of Type-5 arch dam on rigid foundation rock for linear (a) and nonlinear (b) analysis.

and that from the nonlinear analysis of the dam is shown in Figure 7(b). The maximum crest displacement increases from 6.06 cm to 24.43 cm due to hydrodynamic effects in the linear analysis of the dam, and from 6.79 cm to 25.69 cm in the nonlinear analysis of the dam with the curve description method. The difference between the maximum crest displacements obtained from the linear and nonlinear analysis is 12% for the empty reservoir and 5% for the full reservoir. However, the time-histories of the crest displacements in Figure 7 are similar. This is because the deformations of the dam concrete remain in the elastic range for the assumed stress-strain relationship in Figure 2, the other material properties used in the analyses and the selected earthquake loading.

The maximum tensile stresses were obtained on both the upstream and downstream dam face in the directions x-x, y-y and z-z. However, the stresses on the upstream face of the dam only were presented. The stresses were calculated at the centroid of the elements and presented in the form of stress contours. The maximum tensile stresses obtained from the linear analysis of the dam on the upstream dam face in the directions x-x, y-y and z-z are shown in Figure 8, and those obtained from nonlinear analysis of the dam are shown in Figure 9. In the linear analysis of

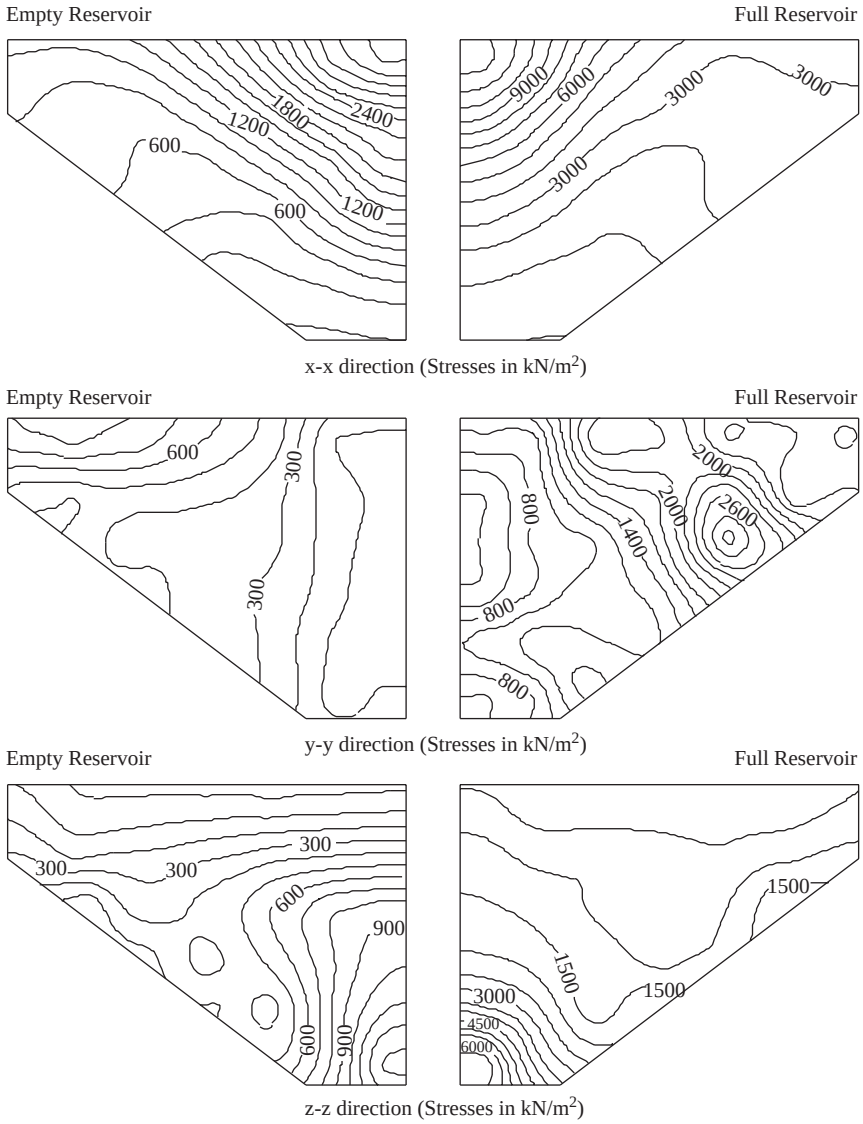

Figure 8. Envelopes of the maximum tensile stresses on upstream face of Type-5 arch dam on rigid foundation rock for linear analysis.

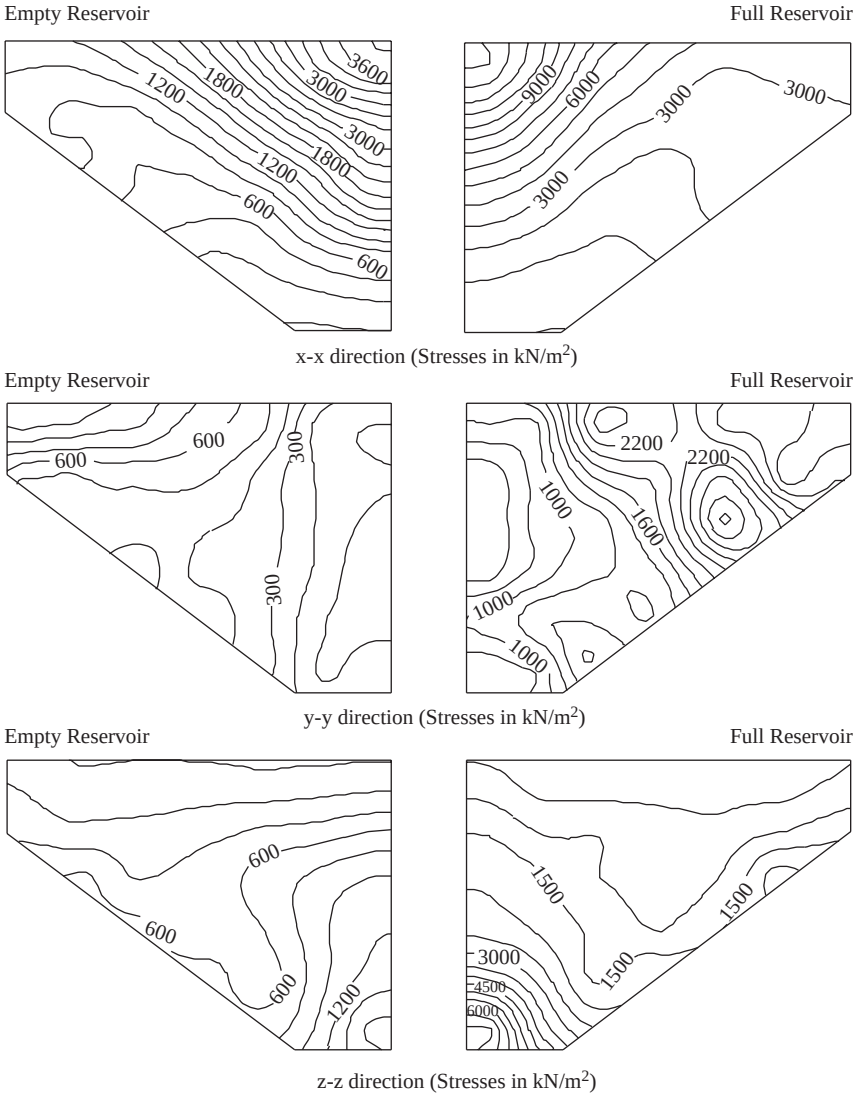

Figure 9. Envelopes of the maximum tensile stresses on upstream face of Type-5 arch dam on rigid foundation rock for nonlinear analysis.

the dam, the stresses in the direction x-x increase from 3381 kN/m^2 to 12365 kN/m^2, the stresses in the direction y-y increase from 823 kN/m^2 to 3117 kN/m^2 and the stresses in the direction z-z increase from 1319 kN/m^2 to 6886 kN/m^2 on the upstream face. In the nonlinear analysis of the dam, the stresses in the direction x-x increase from 3718 kN/m^2 to 13034 kN/m^2, the stresses in the direction y-y increase from 947 kN/m^2 to 3129 kN/m^2 and the stresses in the direction z-z increase from 1643 kN/m^2 to 7079 kN/m^2 on the upstream face.

A large portion of the upstream and downstream faces of the dam is affected by excessive tensile stresses due to hydrodynamic effects in both the linear and the nonlinear analysis. The overstressed areas of the dam are the base of the dam and the portions along the abutment. The tensile stresses in the direction x-x are larger than those in the directions y-y and z-z on both the upstream and downstream faces of the dam. In addition, when the stresses in the direction x-x are examined, it is possible to understand the arch action on the dam response. This condition clearly shows the arch action at the dam response. It is apparent that dam-water interaction has greater influence on both the linear and nonlinear responses of the arch dam.

Response of the Type-5 arch dam on flexible foundation rock

The time-history of displacements obtained from the linear analysis of the dam at the crest of the Type-5 arch dam on flexible foundation rock with both an empty and a full reservoir is presented in Figure 10(a), and that from the nonlinear analysis of the dam is presented in Figure 10(b). The maximum crest displacement increases from 12.80 cm to 33.35 cm due to hydrodynamic effects in the linear analysis of the dam, and from 14.52 cm to 35.02 cm in the nonlinear analysis of the dam with the curve description method. The difference between the maximum crest displacements obtained from the linear and nonlinear analysis is 13% for the empty reservoir and 5% for the full reservoir. In the same way as the response of the Type-5 arch dam on rigid foundation rock, the time-histories of the crest displacements in Figure 10 are similar. This is also because the deformations of the dam concrete remain in the elastic range.

The maximum tensile stresses were also obtained on both the upstream and downstream dam faces in the directions x-x, y-y and z-z. However, the stresses on the upstream face of the dam only were presented. The stresses were calculated at the centroid of the elements and presented in the form of stress contours. The maximum tensile stresses obtained from linear analysis of the dam on the upstream dam face in the directions x-x, y-y and z-z are shown in Figure 11, and those obtained from nonlinear analysis of the dam are shown in Figure 12. In the linear analysis of the dam, the stresses in the direction x-x increase from 5775 kN/m^2 to 14612 kN/m^2, the stresses in the direction y-y increase from 1952 kN/m^2 to 4438 kN/m^2 and the stresses in the direction z-z increase from 3476 kN/m^2 to 6895 kN/m^2 on the upstream face. In the nonlinear analysis of the dam, the stresses in the direction x-x increase from 6340 kN/m^2 to 15457 kN/m^2, the stresses in the direction y-y increase from 2106 kN/m^2 to 4947 kN/m^2 and the stresses in the direction z-z increase from 3914 kN/m^2 to 7038 kN/m^2 on the upstream face.

By comparing these results with those for the dam on rigid foundation rock, it can be seen that the effects of foundation flexibility significantly affect the dam response. The effects of dam-water interaction in the linear and nonlinear response of the dam to earthquake ground motion are qualitatively similar for rigid and flexible foundation rock. In general, hydrodynamic effects influence the distribution of the maximum tensile stresses for the dam in a similar manner whether the foundation rock is flexible or rigid. It is obvious that dam-water interaction with flexible foundation rock has a greater influence on the linear and nonlinear response of the arch dam.

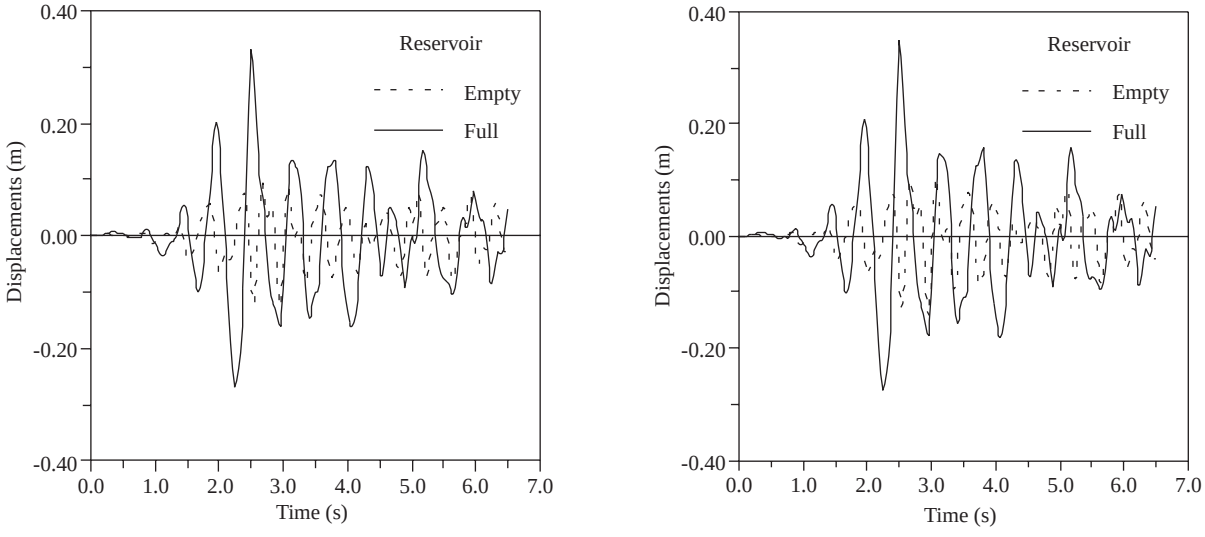

(a) Linear Analysis

(b) Nonlinear Analysis

Figure 10. The time history of displacements at the crest of Type-5 arch dam on flexible foundation rock for linear (a) and nonlinear (b) analysis.

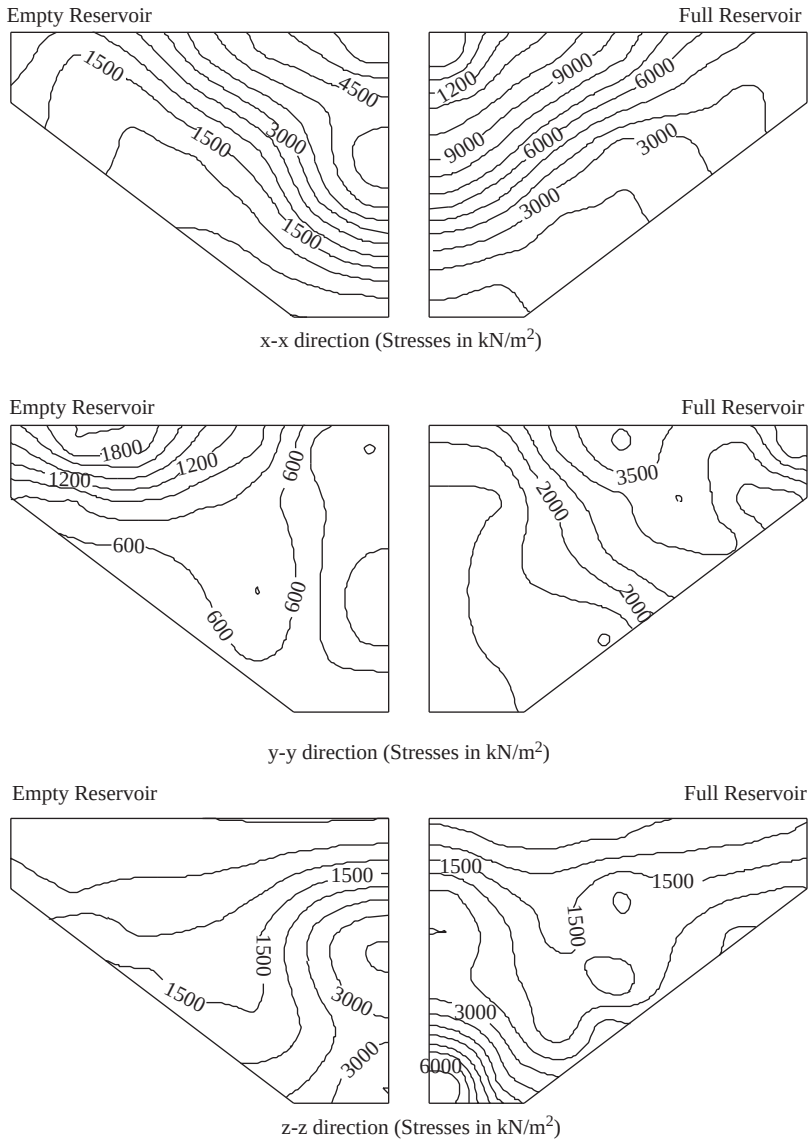

Figure 11. Envelopes of the maximum tensile stresses on upstream face of Type-5 arch dam on flexible foundation rock for linear analysis.

Conclusions

Dam-water, dam-foundation rock and dam-water-foundation rock interactions on the linear and nonlinear responses of a selected arch dam to earthquake ground motion were investigated in this study. The hydrodynamic effects on the dynamic response of a selected arch dam are examined by modeling water in the reservoir with 8-noded Lagrangian fluid finite elements. The step-by-step integration is used to solve the dynamic equations of motion.

The deformations of the dam concrete remain in the elastic range for the assumed stress-strain relationship in Figure 2, the other material properties used in the analyses and the selected earthquake loading. However, it is obvious that hydrodynamic effects considerably affect the linear and nonlinear responses of the dam to earthquake ground motion. In addition, it is shown that the step-by-step integration technique may be efficient in the linear and nonlinear analyses of the response of arch dams to earthquake ground motion and water in the reservoir can be successfully represented by 3-dimensional 8-noded Lagrangian fluid elements.

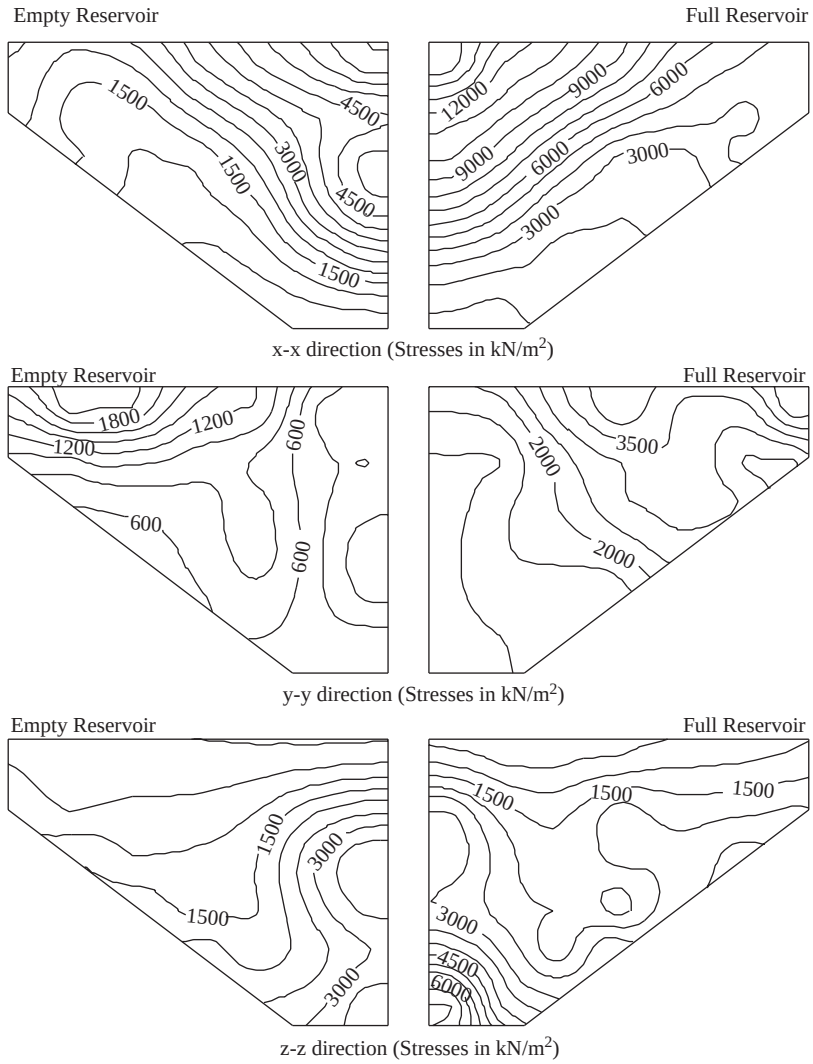

Figure 12. Envelopes of the maximum tensile stresses on upstream face of Type-5 arch dam on flexible foundation rock for nonlinear analysis.

In addition to the conclusions, the following findings from the analyses in this study can be used in the evaluation of the earthquake response of an arch dam:

Both the hydrodynamic and the foundation flexibility effects significantly increase the linear and nonlinear responses of the dam to earthquake ground motion.

The effects of dam-water interaction on the linear and nonlinear responses of the dam to earthquake ground motion are qualitatively similar to those for rigid and flexible foundations.

The hydrodynamic effects influence the distribution of the maximum tensile stresses on the upstream and downstream faces of the dam similarly, whether the foundation rock is flexible or rigid.

Dam-water interaction has more influence on the response of the dam with a flexible foundation than on that of the dam on a rigid foundation in both linear and nonlinear analyses.

A large portion of the upstream and downstream faces of the dam is affected by the excessive tensile stresses due to hydrodynamic effects for both the linear and the nonlinear analyses.

The overstressed areas of the dam are the base of the dam and the portions along the abutment. The tensile stresses on both upstream and downstream faces of the dam in the direction x-x are larger than those in the directions y-y and z-z.

Acknowledgments

The study presented in this paper has been supported by the Turkish Earthquake Foundation under Grant 98-AP-110. We would like to gratefully acknowledge this support. We are also grateful to Professor Rifat Yarar, president of the Turkish Earthquake Foundation, for his encouragement and interest in the project.

Symbols

P	pressures equal to mean stresses
ρ_f	mass density of the fluid
C_{11}	bulk modulus of the fluid
C_{22}, C_{33}, C_{44}	constraint parameters
ε_v	volumetric strain of the fluid
U_{fx}, U_{fy}, U_{fz}	displacement components in the Cartesian axes x, y and z
w_x, w_y, w_z	rotations about the Cartesian axes x, y and z
P_x, P_y, P_z	rotational stresses
σ_f	stress vector of the fluid
$\mathbf{e}_f$	strain vector of the fluid
$\mathbf{C}_f$	elasticity matrix of the fluid
π_e	total strain energy of the fluid system
π_s	potential energy of the fluid system due to the surface motion
T	kinetic energy of the fluid system
$\mathbf{U}_{sf}$	displacement vector of the free surface of the fluid system
$\dot{\mathbf{U}}_f$	velocity vector of the fluid system
$\ddot{\mathbf{U}}_f$	vacceleration vector of the fluid system
$\mathbf{K}_f$	stiffness matrix of the fluid system
$\mathbf{S}_f$	stiffness matrix of the free surface of the fluid system
$\mathbf{M}_f$	mass matrix of the fluid system
$\mathbf{K}_f^*$	system stiffness matrix including the free surface stiffness
$\mathbf{R}_f$	time-varying nodal force vector for the fluid system
U_n	normal component of the interface displacement
$\mathbf{M}_c$	mass matrix for the coupled system
$\mathbf{C}_c$	damping matrix for the coupled system
$\mathbf{K}_c$	stiffness matrix for the coupled system
$\mathbf{U}_c$	displacement vector of the coupled system
$\dot{\mathbf{U}}_c$	velocity vector of the coupled system
$\ddot{\mathbf{U}}_c$	acceleration vector of the coupled system
a_g	vector of ground acceleration
Δt	time increment
θ	the parameter determining the accuracy and stability properties of the Wilson-θ method is always greater than 1
s_{ij}	incremental deviatoric stresses
g_{ij}	incremental deviatoric strains
σ_m	incremental mean stress
e_m	incremental mean strain
E	elasticity modulus
ν	Poisson ratio
K	bulk modulus
K_{LD}	loading bulk modulus
K_{UN}	unloading bulk modulus
G	shear modulus
G_{LD}	loading shear modulus
G_{UD}	unloading shear modulus
$e_{\min}$	minimum mean strain ever reached during the solution
ω_i and ω_j	ith and jth mode frequencies of the system
ξ	damping ratio
a_0 and a_1	Rayleigh damping constants

References

Akkaş, N., Akay, H.U. and Yılmaz, Ç., "Applicability of General-Purpose Finite Element Programs in Solid-Fluid Interaction Problems", Computers and Structures, 10, 773-783, 1979.

Bathe, K.J., Finite Element Procedures in Engineering Analysis, Prentice-Hall, New Jersey, 1996.

Bathe, K.J., Wilson, E.L. and Iding, R., NONSAP: A Structural Analysis Program for Static and Dynamic Response of Nonlinear Systems, Structural Engineering and Structural Mechanics, Department of Civil Engineering, Report No. UC SESM 74-3, University of California, Berkeley, California, 1974.

Calayır, Y. and Dumanoğlu, A.A., "Static and Dynamic Analysis of Fluid and Fluid-Structure Systems by the Lagrangian Method", Computers and Structures, 49, 625-632, 1993.

Calayır, Y., "Dynamic Analysis of Concrete Gravity Dams Using Eulerian and Lagrangian Approaches",

PhD Thesis, Karadeniz Technical University, Graduate School of Natural and Applied Sciences, Trabzon, 1994 (in Turkish).

Calayir, Y., Dumanoğlu, A.A. and Bayraktar, A., "Earthquake Analysis of Gravity Dam-Reservoir Systems Using the Eulerian and Lagrangian Approaches", Computers and Structures, 59, 877-890, 1996.

Chopra, A.K., Wilson, E.L. and Farhoomand, I., "Earthquake Analysis of Reservoir-Dam Systems", Proceedings of the Fourth World Conference on Earthquake Engineering, Santiago, Chile, 2, 1-10, 1969.

Chopra, A.K., Dynamics of Structures, Prentice-Hall, New Jersey, USA, 1995.

Clough, R.W. and Penzien, J., Dynamics of Structures, Second Edition, McGraw-Hill Book Company, Singapore, 1993.

Fok, K.L. and Chopra, A.K., "Hydrodynamic and Foundation Flexibility Effects in Earthquake Response of Arch Dams", Journal of Structural Engineering, 112, 1810-1828, 1986.

Greeves, E.J., The Modelling and Analysis of Linear and Nonlinear Fluid-Structure Systems with Particular Reference to Concrete Dams, PhD Thesis, Department of Civil Engineering, University of Bristol, 1991.

Hamdi, M.A., Ousset, Y. and Verchery, G., "A Displacement Method for the Analysis of Vibration of Coupled Fluid-Structure Systems", International Journal for Numerical Methods in Engineering, 13, 139-150, 1978.

ICE, Arch Dams: A Review of British Research and Development, Proceedings of the Symposium Held at the Institution of Civil Engineers, London, England, 1968.

Olson, L.G. and Bathe, K.J., "A Study of Displacement-Based Fluid Finite Elements for Calculating Frequencies of Fluid and Fluid-Structure Systems", Nuclear Engineering and Design, 76, 137-151, 1983.

Perumalswami, P.R. and Kar, L., "Earthquake Behavior of Arch Dams-Reservoir Systems", Fifth World Conference on Earthquake Engineering, Rome, 1973.

Shugar, T.A. and Katona, M.G., "Development of Finite Element Head Injury Model", Journal of the Engineering Mechanics Division, ASCE, 101, EM3, 11367, 223-239, 1975.

Tan, H. and Chopra, A.K., "Earthquake Analysis of Arch Dams Including Dam-Water-Foundation Rock Interaction", Earthquake Engineering and Structural Dynamics, 24, 1453-1474, 1995.

Tan, H. and Chopra, A.K., "Dam-Foundation Rock Interaction Effects in Earthquake Response of Arch Dams", Journal of Structural Engineering, 122, 528-538, 1996.

Westergaard, H. M., "Water Pressures on Dams during Earthquakes", Transactions, ASCE, 98, 1835, 418-433, 1933.

Wilson, E.L. and Khalvati, M., "Finite Elements for the Dynamic Analysis of Fluid-Solid Systems", International Journal for Numerical Methods in Engineering, 19, 1657-1668, 1983.

Zienkiewicz, O.C. and Bettes, P., "Fluid-Structure Dynamic Interaction and Wave Forces. An Introduction to Numerical Treatment", International Journal for Numerical Methods in Engineering, 13, 1-16,1978.

Zienkiewicz, O.C. and Taylor, R.L., The Finite Element Method, Vol. I, McGraw-Hill, 1989.